This is a preprint of a paper that appeared in the Proceedings of IEEE International Symposium on Robot and Human Interactive Communication (RO-MAN), 2014, Edinburgh

Comparison of Trajectory Generation Methods for a Human-Robot Interface based on Motion Tracking in the Int^{2}Bot

F. Schültje[1], P. Beckerle[2,5], M. Grimmer[3], J. Wojtusch[4,5], S. Rinderknecht[2]

***Abstract*— The acceptance of artificial devices like prostheses or other wearable robots requires their integration into the body schemas of the users. Different factors induce, influence and support the integration and acceptance of the device that substitutes or augments a part of the body. Previous studies have shown that the inducing and maintaining factors are visual, tactile and proprioceptive informations as well as their multisensory integration. This paper describes the vision-based part of the human-robot interface in the Int^{2}Bot, which is a robot for the investigation of lower limb body schema integration during postural movements. The psychological approach and the technical setup of the robot, which is designed to imitate postural movements in the sagittal plane to imitate the human subject while performing squats, are outlined. To realize the imitation, an RGB-D sensor, in form of a Microsoft Kinect, is used to capture the subjects motions without contact and thereby avoid disturbances of body schema integration. For generation of the desired joint trajectories to be tracked by the control algorithm, different methods like an extended Kalman filter, inverse kinematics, an inverse kinematics algorithm using Jacobian transpose and approaches based on kinematic assumptions are presented, evaluated and compared based on human data. Benchmarking the results with data acquired using a professional motion capturing system shows that best overall joint angle estimations are achieved with the extended Kalman filter. Finally, the practical implementation within the robot is presented and the tracking behavior using the trajectories generated with the extended Kalman filter are analyzed.**

I. INTRODUCTION

After amputation, major psychological changes of people with limb loss concern their body images and body schemas [1]. While the body image means the psychological experience of the own body, the body schema is a subconscious, neurophysiological and multisensory representation of its characteristics [2], [3] and is thus linked to the sense of having control over the own body. Successful functional adaptation to the prosthesis is assumed to be reached, if artificial and intact extremities are equally integrated and represented in both, the body schema and body image [2]. Deficits in this process related to human information processing can be observed as feelings of unrealistic body parts or as phantom sensations [4]. The duration of the re-regulation process of such sensations is found to be about four years [2], [5] and the mentioned symptoms seem to be due to disturbances in the experience of the body schema and image [3]. Manipulation of the body schema is a promising approach to improve prosthetic intervention due to experimental investigations of the Rubber Hand Illusion (RHI). These investigations can be performed with a passive rubber hand [6] or with a robotic hand prosthesis [7]. First investigations on transferring the Rubber Hand Illusion to the lower limbs in terms of a Rubber Foot Illusion show significant changes in survey data while results differ regarding the proprioceptive drift [8], [9]. The Int^{2}Bot that is subject of this paper represents a robotic concept to perform such experiments during lower limb motion as proposed in [10]. Therefore, it imitates human postural motions based on data acquired with a Microsoft Kinect camera. The noise of the Kinect RGB-D sensor measurement and the derived Cartesian human skeleton joint positions obtained by the NITE algorithms [11] is fairly high with up to $40\,\mathrm{cm}$ standard deviation [12], [13], [14], [15], [16]. Alternative approaches to human motion tracking are particle filters using RGB-D data [17], extended Kalman filters (EKF) fusing RGB-D and gyroscope data [18] or EKF with marker-based measurement [19]. This paper deals with the vision part of the human-robot interface in the Int^{2}Bot using an Microsoft Kinect sensor. For motion tracking of the human leg, the NITE algorithms [11] , which are optimized for a frontal view of the sensor, are utilized. Section II briefly explains the psychological test design and the robotic setup. Furthermore, the aquisition of human motion data using the Kinect and the Qualisys system are presented in Section III. In Section IV, different algorithms for trajectory generation are described and the extended Kalman filter, the inverse kinematics and an algorithm using the Jacobian transpose are pointed out. Furthermore, the results of the different algorithms are compared and experimental results are shown. In Section V, the implementation on robot and experimental results are shown. Finally, a conclusion and an outlook are given in Section VI.

II. CONCEPT

The test design proposed by the authors to investigate Rubber Leg Illusion (RLI) and its maintaining factors during movement using the robotic setup from [10], [20] is shown in Figure 1. It aims at examining the RLI during postural movements. As a lack of satisfaction in postural motor functioning irrespective of the prosthesis technology and a

*This work was funded by Forum for Interdisciplinary Research of Technische Universität Darmstadt.

[1] Institute for Anthropomatics and Robotics, Karlsruhe Institute of Technology, Karlsruhe, Germany, fabian.schueltje@kit.edu

[2] Institute for Mechatronic Systems in Mechanical Engineering, Technische Universität Darmstadt, Darmstadt, Germany lastname@ims.tu-darmstadt.de

[3] Locomotion Laboratory, Technische Universität Darmstadt, Darmstadt, Germany, grimmer@sport.tu-darmstadt.de

[4] Simulation, Systems Optimization, and Robotics Group, Department of Computer Science, Technische Universität Darmstadt, Darmstadt, Germany wojtusch@sim.tu-darmstadt.de

[5] *Member, IEEE*

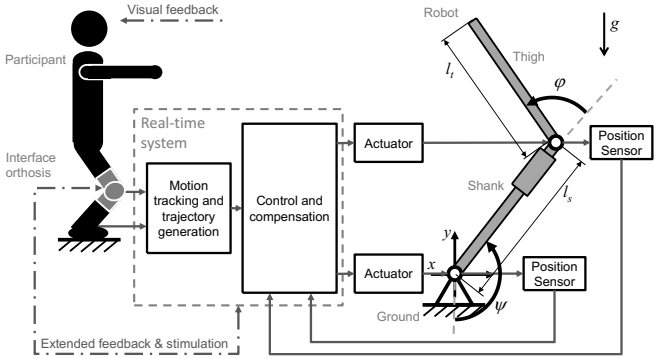

Fig. 1. Functional concept of the Int^{2}Bot based on [20]. Solid arrows represent signal and power flow in the control loop. Dash-dotted arrows indicate multi-sensory feedback channels.

significant correlation between appearance as an indicator of subjective body schema integration is correlated with postural movement satisfaction [20], [21]. The test design from [10] requires the robot to imitate human postural motions, while the participant stands close to it, to investigate influences like synchronous and asynchronous feedback motivated by [22] or the impact of distance between participant and robot motivated by [23]. Furthermore, proprioceptive drift and the questionnaire from [23] are analyzed as well as control variables like ambient conditions. Robot motion is limited to squat motions of one human leg in sagittal plane. At the same time, the imitated leg of the participant is hidden to enable the occurrence of a RLI regarding the robot. The functional concept of the Int^{2}Bot according to [10] and possible extensions described in [20] are depicted in Figure 1. The mechanics of the robot mimic appearance and functionality of foot, shank and thigh as well as the knee and ankle joint. A Microsoft Kinect sensor is utilized for contactless motion tracking for the generation of desired trajectories for controlling of the robot to imitate the human. Control and compensation algorithms utilize proprioceptive sensor data from the robot joints and calculate the required actuator inputs. Human experiments are approved by TU Darmstadt ethics committee.

III. DATA ACQUISITION

In Figure 1, data acquisition by the Kinect camera is shown. As a reference, a tracer system is utilized to examine the error caused by the trajectory deviations of the Kinect camera. Since the Int^{2}Bot is intended to be used for investigating RLI during postural movements in sagittal plane, squats are observed in the reference measurements. As squatting movements with a frequency of $0.5\,\mathrm{Hz}$ are required [10], the subject is asked to hold this speed. A metronome is set up to give the subject a reference signal for the squatting speed. Figure 2 shows the reference system for the Kinect sensor and the tracer system. The tracer system is referenced to a L-shaped marker set, which is placed in the area to be tracked, before the experiments. Based on the segments of this marker set, reference axes are determined. Based on the shanks of the L-shape the reference axes including the root point is calculated. The reference axes of the Microsoft Kinect sensor is located in the RGB-sensor. To be able to compare the two measurement systems the axes are aligned with their origin in the subject's right ankle by transformations.

A. Human data acquisition

The concept for the acquisition of the desired trajectories for the control algorithm with a Kinect sensor is introduced in [10]. One main goal of this human-machine interface is to avoid disturbances of the RLI. A contactless motion tracking without markers or other sensing on the human body is aimed for. Therefore, the joint angles of knee and ankle are determined by skeleton tracking of the participant. In contrast to the knee angle, which can easily be determined with the positions of shank and thigh, the vertical vector of the room is additionally necessary to track the ankle angle, as this is not provided by the OpenNI package and PrimeSense NITE middleware [24], [25]. The approach in [10] proposes the calculation of the ankle angle based on the shank position and an estimation of the ground surface with a marker based approach. For the implementation of the concept from [10], the OpenNI package and PrimeSense NITE middleware are combined with a LabVIEW project for motion acquisition [11]. This allows transfer of the desired trajectories from skeleton tracking to the computed torque control. Yet, it does not provide tracking in real time, since only the control algorithm is running in the deterministic loop of the LabVIEW program. The data captured by the Kinect is transferred to a Host-PC via an universal serial bus connection. The Host-PC is connected via local area network to the CompactRIO on which the real time environment is implemented. According to early tests, the best results for tracking the lower limbs are obtained if the Kinect sensor is located in $3\,\mathrm{m}$ distance of the participant and aligned to the saggital plane of the subject, slightly below knee height. The skeleton model of the tracking software is depicted in Figure 2. Here, the coordinates that are available from the software are marked by black dots. Furthermore, the grey-filled dots indicate the coordinates, which are used for joint angle calculation, excluding the torso marker. These coordinates represent the vectors a_r pointing at the right ankle and k_r for the right

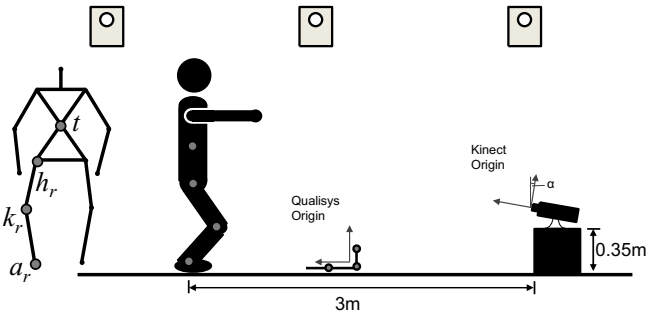

Fig. 2. Skeleton model (left) and test setup with reference systems for Kinect and Qualisys (right).

knee as well as h_r and h_l for the right and left hip. Instead of defining a basis for the calculation of the ankle joint angle using markers, the coordinates a_r, k_r, h_r are used to determine the mean normal vector of the body relatively to the ground, while the subject is standing upright. Assuming the difference in depth distance between the Microsoft Kinect and the ankle, the knee and the hip point is zero while the subject is standing upright. The rotation matrix θ which rotates the orientation of the Microsoft Kinect by the value of α origin is calculated by

$$\theta = \begin{bmatrix} 1 & 0 & 0 \\ 0 & \cos(\alpha) & -\sin(-\alpha) \\ 0 & \sin(\alpha) & \cos(\alpha) \end{bmatrix}. \tag{1}$$

Using this, the differences in depth $x_a - x_k$, $x_a - x_h$ and $x_k - x_h$ are minimized after the test rig is set up but before the actual measurement.

B. Human reference data

To quantify the precision of the Kinect sensor, a dataset for comparison was measured. A motion capture system (Qualisys, Oqus 3+ cameras) is used to record squads in parallel to the Kinect. The motion capture system (240Hz) uses 8 times the measurement frequency of the Kinect sensors (30Hz). 10 cameras were placed around the subject to determine the 3D coordinates of 18 reflective markers. Markers are placed at prominent body locations to determine joints and segments similar to the segmented model used by the Kinect skeleton tracking. To determine the position of the head, a marker was placed between the eyebrows. Trunk position is determined by placing markers at the neck (7th cervical vertebra), the chest (sternum) and the lower back (sacrum). Leg placement is measured by markers placed at the hip (trochanter major), the knee (2 cm proximal of the lateral joint space on the lateral femoral condyle), a marker at the ankle (lateral malleolus) and a marker at the toe (5th metatarsophalangeal joint). Arm alligment was measured by a marker placed on the shoulder (acromeon), the elbow (olecranon) and the wrist (processus styloideus ulnae). Arm and leg markers are placed on both sides of the body. In the calibration process, the Qualisys system determined an error of about 1.08 mm when measuring the distance of 2 markers, placed on the calibration wand, moved through the calibration area.

IV. METHOD COMPARISON

This section deals with the comparison of diffrent algorithms for generating suitable trajectories for the angles from noisy Kinect joint position data. After presenting the algorithms to be compared, criteria for their assessment are defined. In the last part of this section, the results of the algorithms using the data from the Kinect camera and the comparison with the Qualisys measurments are shown and discussed.

A. Methods

First measurements using the Kinect camera showed that the limb length of the estimated shank and thigh varies over time. Based on these first findings all investigated methods are implemented in two versions. One version assuming pre-defined segment lengths based on an intial static measurement of the subject and another with dynamic length adjustment. For the latter case, the algorithms are extended considering varying joint distances of the actual time step by by calculating the differences of the joint positions.

Vector operations

In [18], the knee angle is calculated using vector operations. For the determination of the joint angles from the skeleton coordinates, the vectors of shank $p_1 = a_r - k_r$ and thigh $p_2 = h_r - k_r$ are calculated. The angle between the vectors p_1 connecting knee and foot and p_2 connecting knee and hip is caculated using

$$\psi = \pi - \cos^{-1}\left(\frac{p_1 \cdot p_2}{||p_1|| \cdot ||p_2||}\right). \tag{2}$$

The angle between the ankle and the horizontal axis of the room is calculated by

$$\varphi = \frac{\pi}{2} - \cos^{-1}\left(\frac{-p_1 \cdot e_3}{||-p_1|| \cdot ||e_3||}\right). \tag{3}$$

Using the normal vector

$$e_3 = \begin{bmatrix} 0 \\ 0 \\ 1 \end{bmatrix}, \tag{4}$$

aligned with the vertical axis of the room by initial manual adjustment through transformation. Based on these calculations different methods with various assumptions are developed. The most simple approach assumes pure vertical movement of the hip point, while another one calculates the hip point from the torso point and a predefined offset. Beyond this, the most complete approach takes into account the inclination of the upper body.

Extended Kalman filter

The extended Kalman filter [26] is a statistic method which is capable to estimate future process variables under the use of system information. In general, the process of the extended Kalman filter can be split into two steps: prediction and update. The implementation proposed in this paper uses the angles of the foot ψ and knee φ as internal state vector $\chi = [\psi\ \varphi]^T$ and a constant position model according to [19]. Based on the internal state vector of the previous step, a prediction of the internal state vector in the actual time step is calculated. Applying the constant position model this prediction is given as follows:

$$\begin{aligned} \chi_k &= f(\chi_{k-1}) \\ \chi_k &= \chi_{k-1}. \end{aligned} \tag{5}$$

This constant position model leads to constant state estimates between the time steps, which is appropriate due to the slow motions of the robot. The matrix of partial derivatives

of f with respect to χ is given by a unity matrix A with a dimension of two calculated by

$$A_{i,j} = \frac{\partial f_i}{\partial \chi_j}(\hat{\chi}_{k-1}, u_{k-1}). \tag{6}$$

The covariance of the process is given by a unity matrix Q and the covariance of the measurement is given by a unity matrix R. Based on A, Q, and the covariance P_{k-1} of the previous state, the covariance is projected ahead by

$$P_k^- = A_k P_{k-1} A_k^T + Q_{k-1}. \tag{7}$$

Using the projected state vector and the projected covariance the update step is executed. The positions of the hip and knee joints of the subject are considered, in the measurement matix h, which calculates the Cartesian joint positions from the internal states and corresponds to the kinematic function

$$h(\chi_k) = \begin{bmatrix} l_s \sin(\psi) + l_t \sin(\psi + \varphi) \\ -l_s \cos(\psi) - l_t \cos(\psi + \varphi)) \end{bmatrix}. \tag{8}$$

The matrix of partial derivates of h with respect to the state vector χ is calculated using

$$H_{i,j} = \frac{\partial h_i}{\partial \chi_j}(\widetilde{\chi}_k, 0). \tag{9}$$

For the Int^{2}Bot the resulting H matrix is given by

$$H = \begin{bmatrix} l_s \cos(\psi) + l_t \cos(\psi + \varphi) & l_t \cos(\psi + \varphi) \\ l_s \sin(\psi) + l_t \sin(\psi + \varphi)) & l_t \cos(\psi + \varphi)) \end{bmatrix}. \tag{10}$$

Using this, the Kalman gain is calculated by

$$K_k = P_k^- H_k^T (H_k P_k^- H_k^T + R_k)^{-1}. \tag{11}$$

Next, the internal state is updated using the Kalman gain and the actual measurement of the Cartesian joint positions. The measured Cartesian hip joint positions of the actual time step k are represented by the vector $z_k = [x_{h,k} \quad y_{h,k}]^T$ and the updated internal state by $\hat{\chi}_k$.

$$\hat{\chi}_k = \hat{\chi}_k^- + K_k(z_k - h(\hat{\chi}_k^-, 0)). \tag{12}$$

For the prediction step, covariance is updated by

$$P_k = (I - K_k H_k) P_k^-, \tag{13}$$

where I represents a unity matrix. Measurement noise is taken into account as a diagonal matrix of squared sensor noise of the Microsoft Kinect. For the Int^{2}Bot it is considered as a diagonal matrix with element value of 25. The process noise is determined as a diagonal square matrix by empirical tests with values of 0.25.

Inverse kinematics

The inverse kinematics function, mapping joint to workspace positions, is common in robotics. Here, it is is given by

$$\begin{bmatrix} \psi \\ \varphi \end{bmatrix} = \begin{bmatrix} \tan^{-1}\left(\frac{x_h}{-y_h}\right) - \tan^{-1}\left(\frac{l_t \sin(\phi)}{l_s + l_t \cos(\phi)}\right) \\ \cos^{-1}\left(\frac{x_h^2 + y_h^2 - l_s^2 - l_t^2}{2 l_s l_t}\right) \end{bmatrix}. \tag{14}$$

Using this algorithm, main issues are singular configurations. These singularities occur when the determinant of the direct kinematics equals zero. In the case of the Int^{2}Bot, this occurs if the thigh is aligned with the shank. This means that the knee always have to be in a slightly bent position.

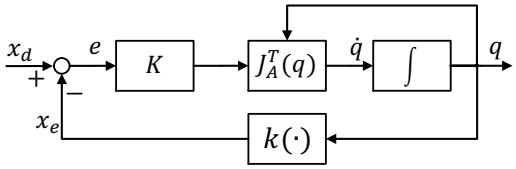

Fig. 3. Inverse kinematics algorithm using Jacobian transpose [27].

Inverse kinematics algorithm using Jacobian transpose

An algorithmic solution of the inverse kinematics problem uses the transposed of the analytical Jacobian to map the measured Cartesian joint positions to the joint angles [27]. Assuming that the Jacobian is square and nonsingular,

$$\dot{q} = J_A^{-1}(q)(\dot{x}_d + Ke), \tag{15}$$

leads to the equivalent linear system $\dot{e} + Ke = 0$. Based on the direct method of Lyapunov the function candidate

$$V(e) = \frac{1}{2} e^T K e, \tag{16}$$

is given to derive an algorithm which ensures error convergence without the requirement of linearization of (15). In this, K is chosen to be a symmetric, positive definite matrix and V is selected in a way that it fulfills $V(e) > 0 \forall\, e \neq 0, V(0) = 0$. Derivation of V leads to

$$\dot{V}(e) = e^T K \dot{\chi}_d - e^T K \dot{\chi}_e. \tag{17}$$

Replacing $\dot{\chi}$ by $J_A(q)\dot{q}$ and $\dot{q}$ by $J_A^T(q)Ke$ leads to

$$\dot{V}(e) = e^T K \dot{\chi}_d - e^T K J_A(q) J_A^T(q) K e. \tag{18}$$

Equation (18) is negative definite and hereby asymptotically stable. Figure 3 illustrates the resulting block scheme. Using this algorithm, issues occur when the hip point lies beyond the area of movement of the Int^{2}Bot. Beyond this area, a solution does not exist and the algorithm will not converge.

B. Assessment Criteria

The mean error between the data generated with the presented algorithms using the Microsoft Kinect and the tracer system Qualisys calculated by

$$\bar{\psi}_{error} = \frac{\sum_{i=1}^{n} \|\psi_{Kinect} - \psi_{Qualisys}\|}{n}. \tag{19}$$

This mean error is used to compare the investigated methods regarding their ability to restore the trajectories. It shows the general accuracy of the methods. Yet, single outliers are not considered in this value due to averaging. Hence, standard deviation is calculated in addition to rate such outliers

$$\sigma = \sqrt{\frac{1}{n-1} \sum_{i=1}^{n} (\chi_i - \bar{\chi})^2}. \tag{20}$$

Using both, the mean error and the standard deviation, the comparison of the algorithms should help to find an appropriate solution for implementation.

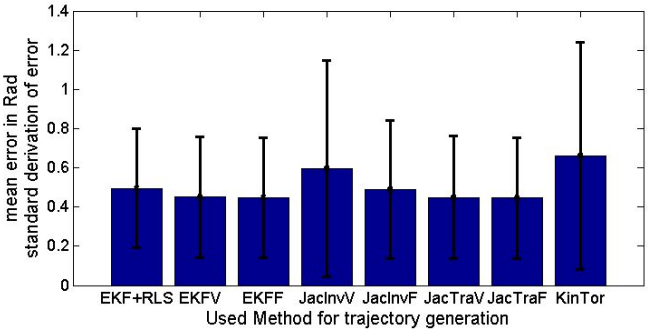

Fig. 4. Comparison of different algorithms

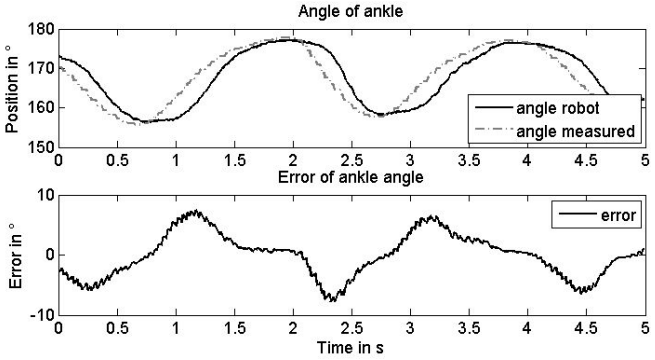

Fig. 5. Angle and error of ankle using the EKF while squatting at approximate $0.5\,\mathrm{Hz}$.

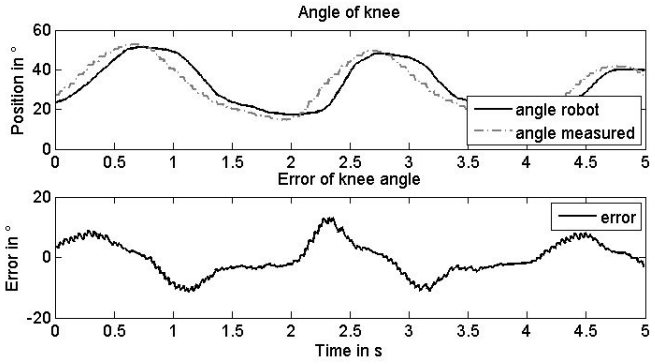

Fig. 6. Angle and error of knee using the EKF while squatting at approximate $0.5\,\mathrm{Hz}$.

C. Results of comparison

Based on equations (19) and (20), the investigated methods are evaluated and compared in this section. The results are shown in Figure 4 using a bar plot of the mean error including the corresponding standard deviations as error bars. From the left, the compared methods are: extended Kalman filter with Recursive Least Squares for segment lengths estimation (EKF+RLS), extended Kalman Filter with variable (EKFV) and fixed (EKFF) segment length, inverse kinematics with variable segment length (InvKinV) and fixed segment length (InvKinF), algorithm using transposed Jacobian with variable (JacTraV) and fix segment length (JacTraF) and vector operations based on the torso point without taking into account the inclination of the upper body. (KinTor). In general, the use of a fixed leg length leads to slightly better results than considering length variations. For inverse kinematics, results obtained by considering a fixed leg length are distinctly better. Best results are achieved using the extended Kalman filter with fixed leg length. Those show a mean error of $0.45\,\mathrm{rad}$ and a standard deviation of $0.31\,\mathrm{rad}$. Anyhow, the measurements are generally dominated by a high standard deviation due to issues of the RGB-D sensor. If the criteria are evaluated specifically for each particular joint, the EKF using fixed leg length shows only third best results for the ankle but the best results for the knee angle. For the ankle the best results are delivered under the use of the vector calculations.

V. IMPLEMENTATION IN INT^{2}BOT

The extended Kalman filter using constant leg lengths and the constant position model showed the best results in offline tests. Therefore, this method is implemented in the Int^{2}Bot. Additionally, the vector operations are implemented as this method provides simple realization and rather good performance in previous tests. All Methods are implemented in combination with elementwise lowpass filtering of the Cartesian skeleton coordinates to reduce the high standard deviation, which the Methods itself could not handle. Both methods require a vertical reference vector, as the Kinect is adjustable in its angle of view and the measured vertical array might not be aligned to the one of the workspace. Therefore, a rotation matrix is implemented to rotate the measurement axes to be aligned to the axes of the workspace as pointed out in section III. During the measurements, the subjects receive an acoustic signal to match their squat frequencies to the one demanded by the experiment. The lowpass filter which smoothens the noise of the Cartesian joint positions is implemented with a cutoff frequency of $1.0\,\mathrm{Hz}$ and used with both trajectory generation methods. Beyond this frequency, sensor noise increases and affects estimation accuracy. Due to this low cutoff frequency, a time shift occurs even at low squat frequencies. In Figure 5 and 6 squatting with frequency of approximate $0.5\,\mathrm{Hz}$ is shown. The maximum position error at the ankle is $7.77\,^\circ$ with a standard deviation of $4.23\,^\circ$, while at the knee the maximum error is $13.98\,^\circ$ and shows a standard deviation of $8.32\,^\circ$. Figure 5 shows the angular position and error of the ankle and Figure 6 the corresponding plots for the knee. Both figures present measurements acquired by using the robotic setup of the Int^{2}Bot, with the subject squatting at approximately $0.5\,\mathrm{Hz}$. The ankle and knee position trajectories generated with the EKF are given by the dash-dotted grey lines and robot positions are presented by solid black lines. The error of the corresponding joint is given in the lower plots. The maximum errors are $7.77\,^\circ$ for the ankle and $13.98\,^\circ$ for the knee. The mean error for the ankle is $2.96\,^\circ$ and $4.79\,^\circ$ for the knee. The delay that can be observed between human and robot motion has several reasons. Kinect processing and the data transfer to the Host-PC causes a time shift of about $90\,\mathrm{ms}$, calculations of the Host-PC and the CompactRIO are discretizised with

a sampling frequency of $100\,\mathrm{Hz}$ causing a time shift of approximately $10\,\mathrm{ms}$ and the local area network connection cause an additional time shift of up to $15\,\mathrm{ms}$. Hence, the total time shift can be approximated to be about $125\,\mathrm{ms}$ and the time shift caused by the lowpass filter might be increased depending on the squat frequency. Although the significant delay caused by transmission and filtering occurs, the methods for trajectory generation show good performance in the operating range around $0.5\,\mathrm{Hz}$. Yet, body schema integration experiments are limited to preliminary tests up to now.

VI. CONCLUSION

In the Int^{2}Bot, robot trajectories are to be generated from human motions captured by a Kinect RGB-D sensor. As sensor data shows high measurement noise, different methods for trajectory generation are investigated in this paper. The inverse kinematics function and the corresponding algorithm using the Jacobian transpose do not show sufficient results in first tests. Since best results are observed using the extended Kalman filter, this approach is implemented in the robot. Furthermore, vector operations in combination with elementwise lowpass filtering are investigated due to the simplicity of this algorithm. Both implemented methods can be used to imitate the postural motions of subjects. With mean errors of $2.96\,^\circ$ in the ankle joint and $4.79\,^\circ$ in the knee joint at squatting frequency of $0.5\,\mathrm{Hz}$, the extended Kalman Filter shows the best results in the experimental examinations. Due to the NITE algorithms for motion capturing and skeleton tracking, Cartesian joint positions show a dynamic error of up to $40\,\mathrm{cm}$. To smoothen those, a lowpass filter cutting of frequencies above $1.0\,\mathrm{Hz}$ is implemented with both presented methods. Despite the significant delay caused by this and the significant standard deviation causing bad measurements, the methods for trajectory generation show good performance in the operating range around $0.5\,\mathrm{Hz}$. Yet, for the application in RLI, the sensor and its interface to the real-time controller should be improved. The remaining limitations of the current robotic setup regarding body schema integration experiments are anyhow mainly caused by insufficient quality of sensor data, since presented methods show good results when they are applied to Qualisys data. In their future works, the authors will investigate new depth sensors. With the extension of the robot by an orthosis as proposed in [20], an optical encoder will be implemented to measure the human knee angle with higher accuracy and incorporate this in the algorithms. Based on the improved motion imitation, psychological experiments on body schema integration will be deduced.

ACKNOWLEDGMENT

The authors thank Bühler Motor GmbH and National Instruments Germany for hardware donations.

REFERENCES

[1] H. Senra, R. Aragao Oliveira, I. Leal, and C. Vieira, "Beyond the body image: a qualitative study on how adults experience lower limb amputation," *Clinical Rehabilitation*, vol. 26, pp. 180 – 191, 2011.

[2] A. Mayer, K. Kudar, K. Bretz, and J. Tihanyi, "Body schema and body awareness of amputees," *Prosthetics and Orthotics International*, vol. 32(3), pp. 363–82, 2008.

[3] S. Gallagher and J. Cole, "Body Schema and Body Image in a Deafferented Subject," *Journal of Mind and Behavior*, vol. 16, pp. 369–390, 1995.

[4] A. I. Goller, K. Richards, S. Novak, and J. Ward, "Mirror-touch Synaesthesia in the Phantom Limbs of Amputees," *Cortex*, vol. http://dx.doi.org/10.1016/j.cortex.2011.05.002, 2012.

[5] C. Murray and J. Fox, "Body image and prosthesis satisfaction in the lower limb amputee," *Disability and rehabilitation*, vol. 24 (17), pp. 925–931, 2002.

[6] M. Botvinick and J. Cohen, "Rubber hands 'feel' touch that eyes see," *Nature*, vol. 391, p. 756, 1998.

[7] B. Rosen, H. H. Ehrsson, C. Antfolk, C. Cipriani, F. Sebelius, and G. Lundborg, "Referral of sensation to an advanced humanoid robotic hand prosthesis," *Scandinavian Journal of Plastic and Reconstructive Surgery and Hand Surgery*, vol. 43, pp. 260–266, 2009.

[8] M. Jokisch, J. Preller, A. Schropp, O. Christ, P. Beckerle, and J. Vogt, "The rubber hand illusion paradigm transferred to the lower limb: A physiological, behavioral and psychometric approach," *International Journal of Psychophysiology*, vol. 85 (3), pp. 421–422, 2012.

[9] O. Christ, A. Elger, K. Schneider, P. Beckerle, J. Vogt, and S. Rinderknecht, "Identification of haptic paths with different resolution and their effect on body scheme illusion in lower limbs," *Technically Assisted Rehabilitation*, 2013.

[10] P. Beckerle, O. Christ, J. Wojtusch, J. Schuy, K. Wolff, S. Rinderknecht, J. Vogt, and O. von Stryk, "Design and control of a robot for the assessment of psychological factors in prosthetic development," *IEEE International Conference on Systems, Man, and Cybernetics*, 2012.

[11] *PrimeSense™ NITE Algorithms 1.5*, PrimeSense Inc, 2011.

[12] T. Dutta, "Evaluation of the Kinect™ sensor for 3-D kinematic measurement in the workplace," *Applied Ergonomics*, vol. 43 (4), pp. 645 – 649, 2012.

[13] F. Menna, F. Remondinoa, R. Battistia, and E. Nocerinoc, "Geometric investigation of a gaming active device," *Proc. of SPIE Vol. 8085*, 2011.

[14] M. R. Andersen, T. Jensen, P. Lisouski, A. K. Mortensen, M. K. Hansen, T. Gregersen, and P. Ahrendt, "Kinect depth sensor evaluation for computer vision applications," AARHUS University Departement of Engineering, Tech. Rep., 2012.

[15] K. Khoshelham and S. O. Elberink, "Accuracy and resolution of kinect depth data for indoor mapping applications," *Sensors*, vol. 12, pp. 1437–1454, 2012.

[16] R. A. Clarka, Y.-H. Puab, K. Fortina, C. Ritchiea, K. E. Websterc, L. Denehya, and A. L. Bryanta, "Validity of the microsoft kinect for assessment of postural control," *Gait & Posture*, vol. 36 (3), p. 372177, 2012.

[17] Z. Li, "Single view human pose tracking," Master's thesis, University of Waterloo, 2013.

[18] A. P. L. Bó, M. Hayashibe, and P. Poignet, "Joint angle estimation in rehabilitation with inertial sensors and its integration with kinect," *IEEE International Conference on Engineering in Medicine and Biology*, 2011.

[19] Q. Fu and M. Santello, "Tracking whole hand kinematics using extended kalman filter," *IEEE International Conference on Engineering in Medicin and Biology*, 2010.

[20] P. Beckerle, F. Schültje, J. Wojtusch, and O. Christ, "Interfaces, User-Feedback and Controls of the Int^{2}Bot for the Investigation of Lower Limb Body Scheme Integration," *IEEE International Symposium on Robot and Human Interactive Communication*, 2014.

[21] O. Christ, P. Beckerle, S. Rinderknecht, and J. Vogt, "Usability, satisfaction and appearance while using lower limb prostheses: Implications for the future," *Neuroscience Letters*, vol. 500 (S1), p. e50, 2011.

[22] E. Lewis and D. M. Lloyd, "Embodied experience: A first-person investigation of the rubber hand illusion," *Phenomenology and the Cognitive Sciences*, vol. 9, pp. 317–339, 2010.

[23] M. R. Longo and P. Haggard, "Sense of agency primes manual motor responses," *Perception*, vol. 38, pp. 69–78, 2009.

[24] "ROS Wiki," 2012. [Online]. Available: http://www.ros.org/wiki

[25] "PrimeSense," 2012. [Online]. Available: http://www.primesense.com/

[26] G. Welch and G. Bishop, "An introduction to the kalman filter," University of North Carolina at Chapel Hill, Tech. Rep., 2006.

[27] B. Siciliano, L. Sciavicco, L. Villani, and G. Oriolo, *Robotics: Modelling, Planning and Control*. Springer, 2009.